Magnetic properties, phase stability, electronic structure, and half-metallicity of $L2_1$-type $Co_2(V_{1-x}Mn_x)Ga$ Heusler alloys

R. Y. Umetsu,[1,*] K. Kobayashi,[2,†] A. Fujita,[2] R. Kainuma,[1] K. Ishida,[2] K. Fukamichi,[1] and A. Sakuma[3]
[1]*Institute of Multidisciplinary Research for Advanced Materials, Tohoku University, 2-1-1 Katahira, 980-8577 Sendai, Japan*
[2]*Department of Materials Science, Graduate School of Engineering, Tohoku University, 6-6-02 Aoba-yama, 980-8579 Sendai, Japan*
[3]*Department of Applied Physics, Graduate School of Engineering, Tohoku University, 6-6-08 Aoba-yama, 980-8579 Sendai, Japan*
(Received 15 March 2007; revised manuscript received 8 November 2007; published 13 March 2008)

Magnetic properties, phase stability, electronic structure, and spin polarization ratio of $L2_1$-type phase in $Co_2(V_{1-x}Mn_x)Ga$ Heusler alloys have been investigated experimentally and theoretically. The experimental magnetic moments M_s at 4.2 K linearly increase with increasing x, *in situ* with the generalized Slater-Pauling rule. The experimental Curie temperature $T_C^{\text{expt.}}$ exhibits a maximum value of about 704 K at $x=0.75$. The latter behavior is comparable to the calculated Curie temperature $T_C^{\text{calc.}}$ from the theoretical effective exchange constant J_0. Although the order-disorder transition temperature $T_t^{L2_1/B2}$ from the $L2_1$- to $B2$-type phase linearly decreases with increasing x, it is relatively high enough in the entire concentration region. The high value of $T_t^{L2_1/B2}$ means that the $L2_1$-type phase can exist stably, which is very important for practical uses. The calculated density of states by the linear-muffitin orbital method with the atomic sphere approximation disclosed that the spin polarization ratio P of the alloy with $x=0.75$ is the highest in the present substituted alloys.

DOI: 10.1103/PhysRevB.77.104422 PACS number(s): 75.50.Cc, 71.20.Be, 75.30.Cr, 71.15.Ap

I. INTRODUCTION

Half-metallic ferromagnets (HMFs) with a high spin polarization ratio P have been investigated intensively as spintronic devices because magnetic tunnel junctions (MTJs) using the HMFs are expected to exhibit a large tunnel magnetoresistance (TMR). The MTJs are required for spintronic devices such as magnetic random access memories and magnetic sensors.[1] From band calculations, it has been pointed out by de Groot *et al.* that the value of P in NiMnSb and PtMnSb alloys with the $C1_b$ (half-Heusler)-type structure is perfect, namely, $P=100\%$.[2] Kübler *et al.* have pointed out that the density of state (DOS) in the minority spin state at the Fermi energy (E_F) vanishes in the Co_2MnAl and Co_2MnSn Heusler alloys.[3] Subsequently, electronic structures and the high values of P for various $L2_1$ (full-Heusler)-type alloys, such as Co_2MnSi and Co_2MnGe, have been calculated.[4–8] Experimental investigations on the TMR of $L2_1$-type alloys have been carried out intensively because the phase stability and the Curie temperature T_C should be high enough from practical viewpoints.[9–13]

According to available band calculations, Co_2CrAl alloy with the $L2_1$-type structure seems to be one of promising candidates for practical applications because E_F is just located at a large peak of the DOS due to the Cr atoms in the majority spin state situated in a gap of the minority spin state.[14–16] However, the expected value of TMR is not yet experimentally obtained for Co_2CrAl films.[17,18] From our systematic studies of the phase stability for $Co_2(Cr_{1-x}Fe_x)Al$ and $Co_2Cr(Al_{1-x}Ga_x)$ alloys, it has been revealed that a phase separation due to a spinodal decomposition, which cannot be suppressed even by water quenching,[19,20] takes place in the lower concentration range of x, resulting in a low value of TMR. This fact strongly suggests that the phase stability is also very important as well as the high values of P and T_C for practical applications of HMFs.

It has been pointed out that a single phase of Co_2CrGa alloy with the $L2_1$-type structure can be obtained by quenching, and experimental magnetic properties are consistent with theoretical calculations, although the precipitation occurs after a long-time annealing.[21,22] The value of T_C of the Co_2CrGa alloy, however, is not so high enough for applicable materials.[21,22] In our previous works, the magnetic properties, phase stability, and electronic structures of the $Co_2(Cr_{1-x}Fe_x)Ga$ alloys were investigated and demonstrated, which the partial substitution of Fe for Cr enhances the phase stability and T_C.[22,23] On the other hand, P decreases with increasing Fe content.[22] Accordingly, it is necessary to develop other Co-based Heusler alloys having more excellent properties for practical applications. Under such recent circumstances, theoretical and experimental investigations for various pseudobinary Heusler alloys have been extensively investigated.[14–16,19–31] However, the phase stability has not been considered in many cases for applicable materials. Systematic experimental researches for the phase stability and magnetic properties of Co_2YZ (Y=Ti, V, Cr, Mn, and Fe, Z=Al and Ga) Heusler alloys have been carried out by Ishikawa[32] and the present authors.[33] It has been pointed out that there is a tendency that the order-disorder transition temperature $T_t^{L2_1/B2}$ from the $L2_1$- to $B2$-type phase decreases with increasing the number of valence electrons.[33] However, $T_t^{L2_1/B2}$ of the Co_2CrAl and Co_2CrGa alloys deviates from this trend, suggesting that the phase stability of the $L2_1$-type phase of the both alloys falls below the mark. Actually, it is consistent with our previous results that the single phase of the $L2_1$-type phase of the Co_2CrAl alloy cannot be obtained.[19,20] In addition, it should be noted that the Heusler alloys are constituted of several kinds of elements, and their phase diagrams are often complicated due to precipitations and phase separations. Compared with a large number of the theoretical reports for the DOS, there are not so many reports on the phase stability for pseudobinary Heusler alloys, restricted to $Co_2(Cr_{1-x}Fe_x)Al$,[19,20] $Co_2(Cr_{1-x}Fe_x)Ga$,[22,23] $Co_2(Mn_{1-x}Fe_x)Si$,[28] and $Co_2Fe(Al_{1-x}Si_x)$.[29] Therefore, it is meaningful to investigate the phase stability and magnetic

properties of the pseudobinary Heusler alloys from practical viewpoints for spintronic devices.

In the present paper, the magnetic properties and phase stability are experimentally investigated for $Co_2(V_{1-x}Mn_x)Ga$ alloy system. Note that the average number of the valence electrons in the alloy with $x=0.5$ corresponds to that in Co_2CrGa alloy. Next, for discussions of the phase stability, we have investigated the order-disorder transition temperature $T_t^{L2_1/B2}$ from $L2_1$- to $B2$-type phase because the height of $T_t^{L2_1/B2}$ closely correlates with the interchange energy between the V(Mn) and Ga atoms. Finally, the electronic structures and spin polarization ratios are theoretically studied.

II. EXPERIMENTAL PROCEDURE

Several kinds of ingots of the $Co_2(V_{1-x}Mn_x)Ga$ alloys were made by arc and levitation-meltings under an argon atmosphere. The specimens cut out from the ingots were annealed at 1373 K for 72 h, and subsequently quenched into ice water. The compositions of the samples were determined with an electron probe microanalyzer and confirmed that the deviation from the nominal composition was less than 1 at. %. From x-ray powder diffraction (XRD) measurement and transmission electron microscopic (TEM) observation, the crystal structure of all the specimens was identified as the $L2_1$-type single phase in the entire concentration range of x. In order to calibrate the lattice constant, powdered Si was mixed with each powdered specimen for reference. The differential scanning calorimetric (DSC) measurement was carried out to evaluate the order-disorder transition temperature. The magnetic measurements were performed with a superconducting quantum interference device magnetometer at low temperatures and with a vibrating sample magnetometer at high temperatures.

III. THEORETICAL MORPHOLOGY OF CALCULATIONS

Within the framework of the local-spin-density functional approximation (LSDFA),[34–36] we employ the tight-binding linear-muffin-tin orbital (TB-LMTO) method in order to treat properly the substitutional disorder under the coherent potential approximation (CPA). The virtue of adopting the TB-LMTO method enables us to evaluate the Green functions which are necessary to calculate the effective exchange constant given below.

The effective exchange constant J_0 is given by the following expression within the linear-muffin-tin orbital (LMTO) scheme:[37,38]

$$J_0 = -\frac{1}{4\pi}\,\mathrm{Im}\int^{E_F} d\omega\,\mathrm{Tr}_{lm}[\Omega_0(\omega)\{g_{00}^{\uparrow\uparrow}(\omega)-g_{00}^{\downarrow\downarrow}(\omega)\} + \Omega_0(\omega)g_{00}^{\uparrow\uparrow}(\omega)\Omega_0(\omega)g_{00}^{\downarrow\downarrow}(\omega)], \quad (1)$$

where $g(\omega)$ is the so-called auxiliary Green function given by $g_{ij}^{\sigma\sigma'}(\omega)=[[p(\omega)-S]^{-1}]_{ij}^{\sigma\sigma'}$, which constitutes of the potential function $p(\omega)$ and the structure constant S defined in the tight-binding LMTO method, and $\Omega_i(\omega)$ is given as $\Omega_i(\omega)\equiv p_i^{\uparrow}(\omega)-p_i^{\downarrow}(\omega)$. Within the local spin-density functional approximation, the potential function $p(\omega)$ can be determined self-consistently. In Eq. (1), the integration is performed up to the Fermi energy E_F and Tr stands for the trace over the orbital (l, m). In the classical Heisenberg model, the Hamiltonian is given by $H=-\Sigma_{i,j}J_{ij}\boldsymbol{e}_i\cdot\boldsymbol{e}_j$, where $\boldsymbol{e}_i$ and $\boldsymbol{e}_j$ denote the unit vectors, and J_0 in Eq. (1) corresponds to $J_0=\Sigma_{i\neq 0}J_{i0}$. Hence, J_0 can be regarded as the effective exchange constant, that is, a magnitude of the exchange field acting on the moment at the 0th site. By using J_0, therefore, we can estimate the Curie temperature $T_C^{\mathrm{calc.}}$ from the following equation within the mean-field approximation for spin systems.[38]

$$T_C^{\mathrm{calc.}}=\frac{2J_0}{3k_B}, \quad (2)$$

where k_B is the Boltzmann constant. From the calculated results, on the other hand, the spin polarization ratio P is obtained from the following expression:

$$P(\%)=\left|\frac{N_{\uparrow}(E_F)-N_{\downarrow}(E_F)}{N_{\uparrow}(E_F)+N_{\downarrow}(E_F)}\right|\times 100, \quad (3)$$

where $N_{\uparrow}(E_F)$ and $N_{\downarrow}(E_F)$ denote the DOS at E_F in the majority and the minority spin states, respectively.

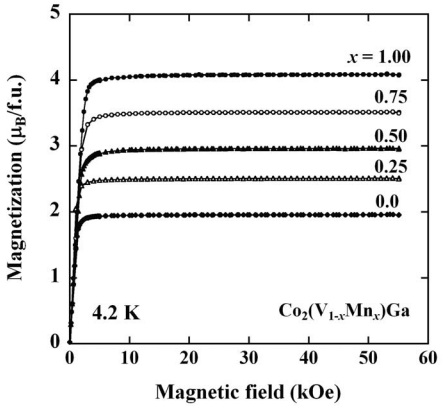

FIG. 1. The magnetization curves at 4.2 K for the $L2_1$-type $Co_2(V_{1-x}Mn_x)Ga$ alloys with $x=0.0$, 0.25, 0.50, 0.75, and 1.00.

IV. RESULTS AND DISCUSSIONS

A. Experimental results

Figure 1 shows the magnetization curves at 4.2 K for several kinds of $L2_1$-type $Co_2(V_{1-x}Mn_x)Ga$ alloys with $x=0.0$, 0.25, 0.50, 0.75, and 1.00. Shown in Fig. 2 is the saturation magnetic moment at 4.2 K M_s for the $L2_1$-type phase in the $Co_2(V_{-x}Mn_x)Ga$ alloys obtained from Fig. 1 and the generalized Slater-Pauling (GSP) rule as a function of the number of the valence electrons Z_t. The corresponding concentration x is also given in the upper x axis. Here, the GSP rule is given by $M_{\mathrm{tot}}=Z_t-24$,[6,7,39–41] with the total spin magnetic moment M_{tot}. Available data (△) for Co_2VGa (Ref. 42) and Co_2MnGa (Ref. 43) alloys are also added in the same figure. In the case of $L2_1$-type Co-based Heusler alloys, the minority band involves 12 electrons per unit cell, that is, 4 electrons of

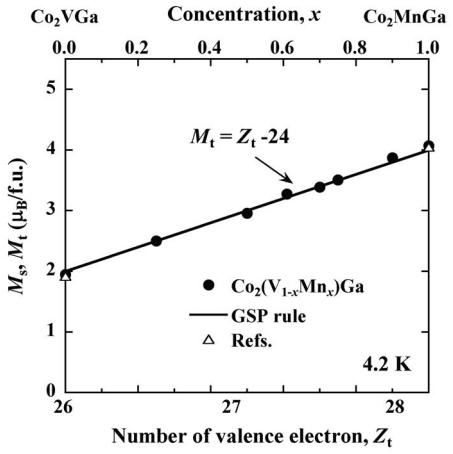

FIG. 2. The saturation magnetic moment at 4.2 K M_s and the generalized Slater-Pauling (GSP) rule for the $L2_1$-type phase in the $Co_2(V_{1-x}Mn_x)Ga$ alloys as a function of the number of the valence electron Z_t, together with literature data (△) (Refs. 42 and 43) The corresponding concentration x is also given in the upper x axis. The solid straight line stands for the GSP rule, $M_{tot}=Z_t-24$ (Refs. 6, 7, and 39–41).

them occupy the low lying s and p bands and 8 electrons are in the Co-like minority d bands.[7] It is well-known that the magnetic moment takes an integral number in the μ_B/f.u., following the GSP rule for the HMFs. The experimental M_s linearly increases with increasing x, in good agreement with the GSP rule, as seen from Fig. 2. It should be noted that the agreement of the experimental saturation magnetic moment with the GSP rule does not always give the identification whether the ferromagnetic material is a HMF or not. In conjunction with the experimental results of the saturation magnetic moment, the total magnetic moment M_{tot} given by the GSP rule and the electronic structures, the theoretical spin polarization ratio and the spin magnetic moment are necessary to discuss with respect to the half-metallicity of ferromagnetic alloys. In the present study, the theoretical spin polarization ratio P will be discussed later.

Figures 3(a) and 3(b), respectively, show the DSC curves and the temperature dependence of the magnetization (M-T) measured in a magnetic field of 5 kOe for the $Co_2(V_{1-x}Mn_x)Ga$ alloys. In these figures, the solid and dashed arrows indicate $T_C^{expt.}$ and the order-disorder transition temperature $T_t^{L2_1/B2}$ from the $L2_1$- to $B2$-type structure, respectively. The value of T_C increases with increasing x, and the values for $x=0.0$ ($\equiv Co_2VGa$) and for $x=1.00$ ($\equiv Co_2MnGa$) are 341 and 686 K, respectively, in good agreement with available values.[42,43] On the other hand, $T_t^{L2_1/B2}$ which is a measure of the phase stability of the ordered $L2_1$-type phase decreases with increasing x, i.e., with increasing number of the valence electrons Z_t.

In the DSC curves, exothermic behaviors are observed at around 1000 K, and there is a tendency that the peaks become sharp with increasing x. Such behaviors would be correlated with structural relaxations during the increase of temperature. For the present Heusler alloy ystem, $T_t^{L2_1/B2}$ was also confirmed by the TEM observations.[44] The lower the alloy composition of x, the higher the order-disorder transition temperature $T_t^{L2_1/B2}$, indicating a high phase stability. Therefore, the specimens quenched from the same temperature exhibit no exothermic behavior.

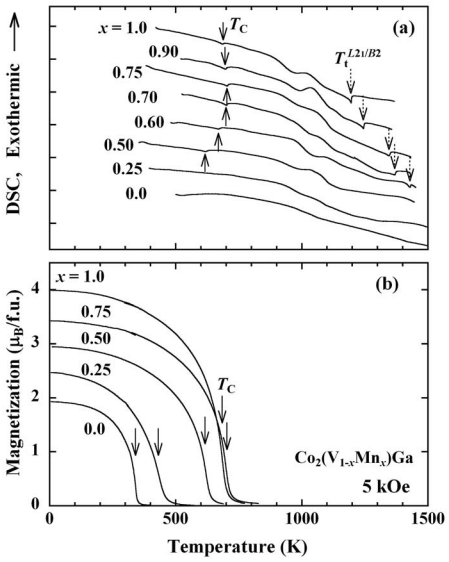

FIG. 3. The (a) DSC curves and the (b) temperature dependence of magnetization measured in a magnetic field of 5 kOe for the $L2_1$-type $Co_2(V_{1-x}Mn_x)Ga$ alloys. The solid and dotted arrows, respectively, indicate the Curie temperature T_C and the order-disorder transition temperature $T_t^{L2_1/B2}$ from the $L2_1$ to the $B2$ phase.

The temperatures of T_C and $T_t^{L2_1/B2}$ obtained from the DSC and M-T curves are plotted against the number of valence electrons in Fig. 4, together with the data for Co_2YGa alloys (Y=Ti, Cr, and Fe).[32] The solid circles and squares indicate the present data, the open circles and squares stand for our previous results,[32,44] and the open triangles are the literature data.[42,43,45] There is a tendency that $T_t^{L2_1/B2}$ monotonically decreases with increasing Z_t except for the Co_2CrGa alloy which exhibits the lowest value among the five alloys. This implies that the phase stability of the $L2_1$-type ordered structure is relatively low. Actually, it has been pointed out that the σ and γ phases easily precipitate in

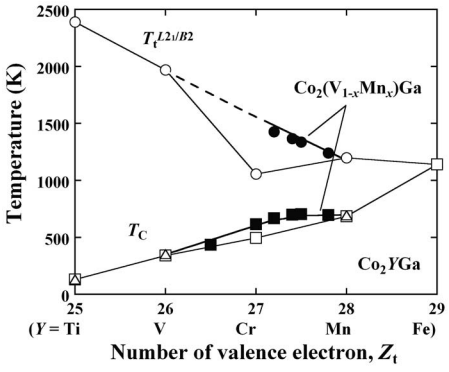

FIG. 4. The Curie temperature T_C and the order-disorder transition temperature $T_t^{L2_1/B2}$ from the $L2_1$ to the $B2$ phase as a function of valence electron numbers, together with available data on T_C for Co_2YGa (Y=Ti, V, and Mn) alloys (△) (Refs. 32 and 42–45). Note that the dashed line gives a linear extrapolation.

the $L2_1$-type phase in the Co_2CrGa alloy.[21,22] Such behaviors are very similar to those in Co_2YAl and Ni_2YAl (Y=Ti, V, Cr, Mn, and Fe) alloys. Concretely speaking, Y=Cr, namely, in Co_2CrAl and Ni_2CrAl alloys, $T_t^{L2_1/B2}$ becomes the lowest, hence no $L2_1$-type single phase can be stabilized due to the phase separation.[19,20,46–48]

According to the Bragg-Williams-Gorsky approximation,[49,50] $T_t^{L2_1/B2}$ of X_2YZ Heusler alloys is given simply from the following relation under the assumption that the degree of order of the X element in the $B2$ phase is perfect at $T_t^{L2_1/B2}$, that is, all the X atoms occupy at the X site at $T_t^{L2_1/B2}$.[51]

$$T_t^{L2_1/B_2} = \frac{3W_{YZ}^{(2)}}{2k_B}, \tag{4}$$

where $W_{YZ}^{(2)}$ is the interchange energy of the Y-Z bonds between the second nearest neighbors and k_B the Boltzmann constant. The $W_{YZ}^{(2)}$ ($=W_{jk}^{(i)}$) is defined as

$$W_{jk}^{(i)} = V_{jj}^{(i)} + V_{kk}^{(i)} - 2V_{jk}^{(i)}, \tag{5}$$

where $V_{jk}^{(i)}$ is the energy of j-k atomic bonding between the ith nearest neighbors. Equation (4) stands for that there is a linear relation between the $T_t^{L2_1/B2}$ and $W_{YZ}^{(2)}$, and that $T_t^{L2_1/B2}$ is only a function of $W_{YZ}^{(2)}$, independent of the other pairwise interactions. It is evident that $W_{\mathrm{VGa}}^{(2)}$ is larger than $W_{\mathrm{MnGa}}^{(2)}$ from the fact that $T_t^{L2_1/B2}$ of the Co_2VGa alloy is higher than that of the Co_2MnGa alloy, as seen from Fig. 4 and our previous data.[32] Since the interchange energy $W_{YZ}^{(2)}$ of the substituted alloys is given by the weighted mean, it is expected to exhibit a linear concentration dependence of $T_t^{L2_1/B2}$ by changing V into Mn in the Y site. Note that the extrapolation is reasonable as given by the dashed line. In Fig. 4, it is interesting to note that $T_t^{L2_1/B2}$ of the $Co_2(V_{0.5}Mn_{0.5})Ga$ with Z_t=27, being the same as that of the Co_2CrGa alloy, is clearly higher than that of the Co_2CrGa alloy. The low $T_t^{L2_1/B2}$ in the Co_2CrGa alloy means the low value of $W_{\mathrm{CrGa}}^{(2)}$ but the reason in such an extremely low value of $W_{\mathrm{CrGa}}^{(2)}$ is not clear at the present stage.

In Fig. 4, T_C of the $L2_1$-type phase in the Co_2YGa (Y=Ti, V, Cr, Mn, and Fe) alloys increases with increasing Z_t and T_C of the Co_2FeGa alloy is high enough and coincides with $T_t^{L2_1/B2}$.[22] It has been reported by our study for the $Co_2(Cr_{1-x}Fe_x)Ga$ alloys that the substituted Fe enhances the magnetic moment of Co, and $T_C^{\mathrm{expt.}}$ linearly increases with increasing Fe content.[22] The concentration dependence of $T_C^{\mathrm{expt.}}$ for the present $Co_2(V_{1-x}Mn_x)Ga$ alloys is not monotonic, but rather convex upward. The maximum $T_C^{\mathrm{expt.}}$ appears in the vicinity of x=0.8, which is higher than that of the $L2_1$-type Co_2CrGa Heusler alloy.[21,22] The details of the concentration dependence of T_C will be discussed in the following section, in connection with the theoretical calculations. The concentration dependence of the room temperature lattice constant of the $Co_2(V_{1-x}Mn_x)Ga$ alloys is shown in Fig. 5. The lattice constant linearly decreases with increasing x. Available data denoted by the symbol (△) for Co_2VGa (Ref. 42) and Co_2MnGa (Ref. 43) are plotted in the same figure. These data are close to the present results.

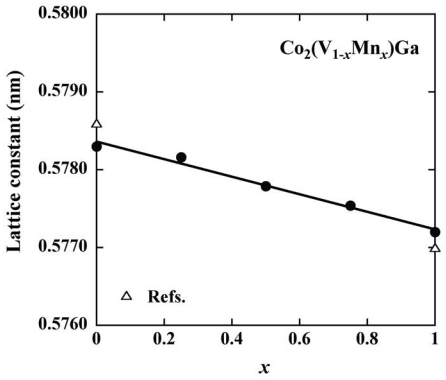

FIG. 5. Concentration dependence of the room temperature lattice constant of the $L2_1$-type phase in $Co_2(V_{1-x}Mn_x)Ga$ alloys, together with available data on Co_2VGa (Ref. 42) and Co_2MnGa (△) (Ref. 43).

B. Theoretical results

The total density of states of the $L2_1$-type $Co_2(V_{1-x}Mn_x)Ga$ (x=0.0, 0.25, 0.50, and 1.00) alloys calculated by the LMTO method with the atomic sphere approximation (ASA) is displayed in Fig. 6. In each panel, the inset shows an expanded scale around the Fermi energy E_F. The upper and lower curves correspond to the majority and the minority spin states, respectively. For the theoretical calculations, the room temperature lattice constants obtained by XRD measurements were used, and the CPA was adopted for the substituted alloys with x=0.25, 0.50, and 0.75. Recently, theoretical calculations for the electronic structure of the $L2_1$-type phase in the Heusler alloys including electron-electron correlation U have been investigated. Depending on calculation methods, different results have been pointed out in several literatures.[27–31,52,53] Although the LMTO-ASA method would be conventional, it seems to be suitable to discuss systematically the aspects of DOS as well as the effective exchange constant J_0 which gives an estimation of the Curie temperature in the present substituted alloys. In addition, it is useful to compare with our previous results for the $Co_2(Cr_{1-x}Fe_x)Ga$ alloys.[22] The values of the spin magnetic moment of each alloy and spin polarization ratio obtained from these theoretical calculations are listed in Table I. A classification scheme for half-metallic ferromagnets has been reported by Coey and Venkatesan,[54] and Felser *et al.*[55] According to their classification, a material exhibiting metallic conductivity and having a semiconducting DOS at one hand spin state is classified into the type I. Among them, the half-metallic Heusler alloys containing first-row transition metals and heavy main-group elements, including the present alloy system, are further divided into the type IA because the transition metal 3d levels are lowered below the 4s band edge due to the hybridization. In all of the present compositions, the large peak at E_F associated with Cr in the $L2_1$-type Co_2CrGa alloy is absent.[21,22] Large peaks of both the Mn and Co in the majority spin states are located in the energy region lower than E_F. Focusing on the minority spin state, E_F in the Co_2VGa alloy (x=0.0) is located at around the upper end of the very low density of states defined as the pseudogap in the

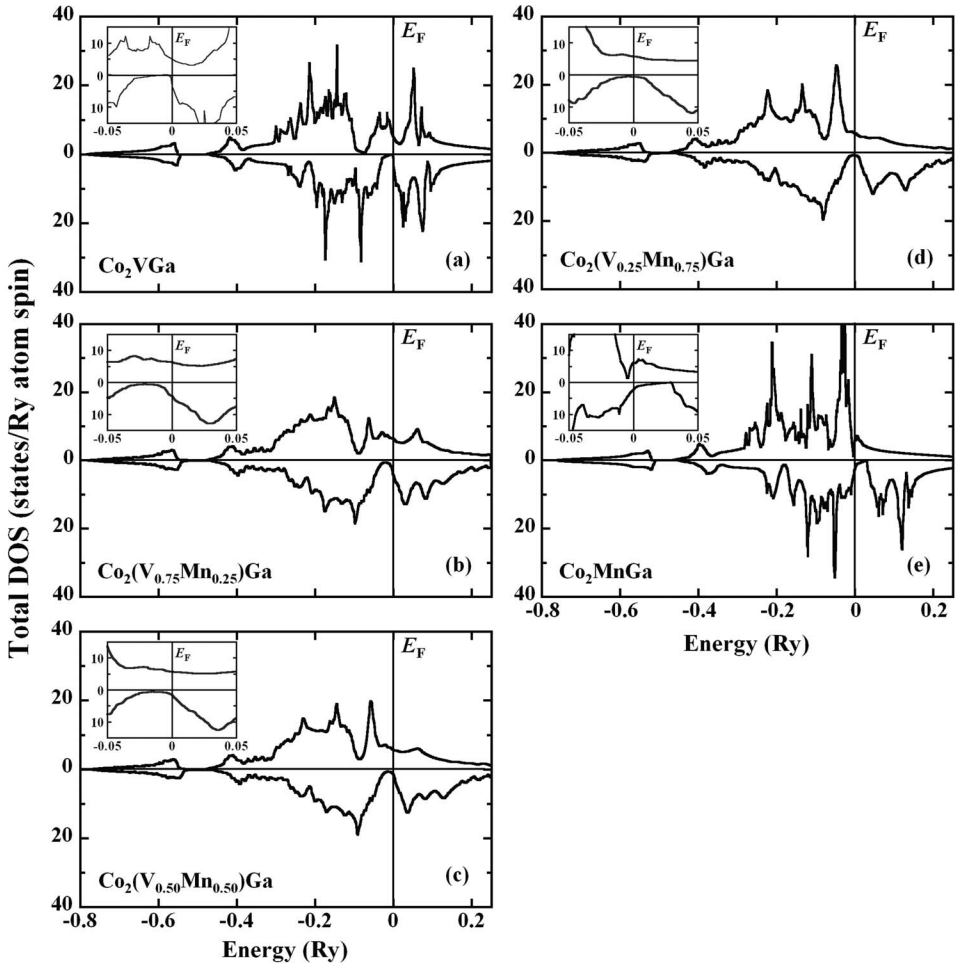

FIG. 6. The total density of states (DOS) for five kinds of alloys with x=(a) 0.0, (b) 0.25, (c) 0.50, (d) 0.75, and (e) 1.00. The upper and lower curves in each panel correspond to the majority and the minority spin states, respectively. The inset is the expanded scale around the Fermi energy E_F in each panel.

present paper. In the Co_2MnGa alloy (x=1.00), E_F contacts with the lower edge of the pseudogap in the minority spin state, and the DOS in the majority spin state is not so high. As a result, P of Co_2MnGa alloy is lowened by about 48%. Theoretical results using the full-potential nonorthogonal local-orbital minimum-basis band structure scheme for the

TABLE I. The experimental room temperature lattice constant, the calculated values of the magnetic moment of each atom $M^{\text{calc.}}$ (μ_B/atom), total spin magnetic moment $M_{\text{tot}}^{\text{calc.}}$ (μ_B/f.u.), the experimental value of the saturation magnetic moment at 4.2 K M_s (μ_B/f.u.), spin polarization ratio P (%), together with the calculated and experimental Curie temperatures $T_C^{\text{calc.}}$ and $T_C^{\text{expt.}}$ (K) of the $L2_1$-type phase in $Co_2(V_{1-x}Mn_x)Ga$ alloys.

$Co_2(V_{1-x}Mn_x)Ga$ (Lattice constant) (nm)	$M_{\text{Co}}^{\text{calc.}}$ (μ_B/atom)	$M_{\text{V}}^{\text{calc.}}$ (μ_B/atom)	$M_{\text{Mn}}^{\text{calc.}}$ (μ_B/atom)	$M_{\text{Ga}}^{\text{calc.}}$ (μ_B/atom)	$M_{\text{tot}}^{\text{calc.}}$ (μ_B/a.u.)	M_s (μ_B/f.u.)	P (%)	$T_C^{\text{calc.}}$ (K)	$T_C^{\text{expt.}}$ (K)
x=0.0 (0.5783)	0.95	0.05	…	−0.02	1.92	1.95	75	247	341
x=0.25 (0.5782)	0.78	−0.01	2.99	−0.03	2.26	2.50	20	737	436
x=0.50 (0.5778)	0.79	−0.13	2.93	−0.05	2.93	2.96	57	858	615
x=0.60	…	…	…	…	…	3.27	…	…	668
x=0.70	…	…	…	…	…	3.39	…	…	700
x=0.75 (0.5775)	0.76	−0.29	2.84	−0.08	3.49	3.51	79	865	704
x=0.90	…	…	…	…	…	3.87	…	…	696
x=1.00 (0.5772)	0.77	…	2.70	−0.13	4.11	4.07	48	778	685

same alloy have been reported by Özdoğan *et al.*[56] The value of P seems to be different from the present result because the position of E_F is slightly different. However, there is no basic contradiction in both the aspects of DOS, and the results of the spin magnetic moments are in good accordance with each other. Furthermore, Sargolzaei *et al.*[57] reported that the theoretical calculation of P for $L2_1$-type Co_2MnGa alloy is 81%, almost twice as high as the present result. Such discrepancy is mainly brought about by the difference in the lattice constants for the calculations. That is, in their calculations, the theoretical lattice constant obtained by the (LSDFA) total-energy calculations was adapted, while the experimental lattice constant listed in Table I was used in the present calculation. In the same way, Sargolzaei *et al.* pointed out that the total magnetic moments are different, depending on the lattice constants determined by experiments and LSDFA calculations.[57]

The DOS for the substituted alloys with $x=0.25$, 0.50, and 0.75 is broad because of the CPA calculations. Among them, the DOS around E_F in the minority spin state is the lowest for $x=0.75$ in Fig. 6(d) and results in P of about 80%, which is the highest in the present substituted alloys of $Co_2(V_{1-x}Mn_x)Ga$. At the present, we are not able to decline that a finite value of the DOS is due to the broadening of the DOS by the CPA or due to the band crossing at E_F.

Collected in Table I are the calculated values of the spin magnetic moment of each atom $M^{\mathrm{calc.}}$ (μ_B/atom), total spin magnetic moment $M_{\mathrm{tot}}^{\mathrm{calc.}}$ (μ_B/f.u.), and spin polarization ratio P (%), the experimental values of the saturation magnetic moment at 4.2 K M_s (μ_B/f.u.), and the calculated and experimental Curie temperatures $T_C^{\mathrm{calc.}}$ and $T_C^{\mathrm{expt.}}$ (K) of the $L2_1$-type $Co_2(V_{1-x}Mn_x)Ga$ alloys. The room temperature lattice constants obtained by x-ray powder diffractions, which were used for the present theoretical calculations, are added to the same table. The largest magnetic moment of Co is about $0.95\mu_B$ in the alloy with $x=0.0$ (Co_2VGa), and the V atoms in this alloy have a small positive magnetic moment of about $0.05\mu_B$. The sign of the magnetic moment of V changes from positive to negative when the Mn atoms are substituted in the V sites, and the magnitude of the moment increases with increasing x. The magnetic moment of Mn, which is almost $3.0\mu_B$ at $x=0.25$, is over three times that of Co and slightly decreases with increasing x. In the case of Ga, the magnetic moment is negative and very small in the entire concentration range of x. The saturation magnetic moment M_s linearly increases with increasing x, as given in Fig. 2, and the theoretical results of the total spin magnetic moment are in good agreement with the experimental data.

For Husler alloys, the magnetic moments have been calculated within the local-(spin)-density approximation [L(S)DA] including the generalized gradient approximation [58] or the electron-electron Coulomb repulsive energy (U). On the basis of the LDA+U calculations, Kandpal *et al.* pointed out, from the systematic theoretical investigations of both Co_2FeSi and Co_2MnSi alloys, that the on-site electron correlation will play an important role in Mn compounds with localized magnetic moments.[52,53] They explain successfully the experimental results of Co_2FeSi alloy. In addition, they suggest that the low value of P in Co_2MnSi is caused by U.[52]

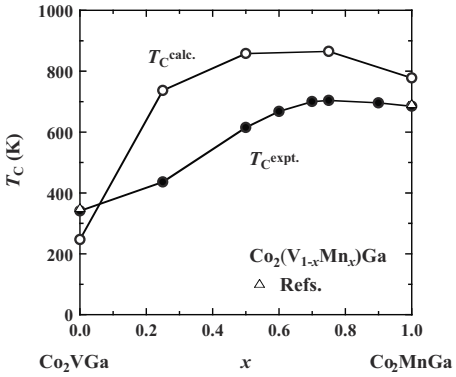

FIG. 7. Concentration dependence of the experimental Curie temperature $T_C^{\mathrm{expt.}}$ and the calculated Curie temperature $T_C^{\mathrm{calc.}}$ of the $L2_1$-type $Co_2(V_{1-x}Mn_x)Ga$ alloys, together with available experimental data for Co_2VGa and Co_2MnGa alloys (△) (Refs. 42 and 43).

On the other hand, very recently, a very high P value of about 90% for Co_2MnSi has been demonstrated by Sakuraba *et al.*[59] For magnetic moment of the Heusler alloys, the contribution from the orbital moments has been pointed out.[57,60] For the spin polarization ratio P, it seems to depend on sample qualities including atomic disorder effects.[25] In such circumstances, it seems to be difficult to select one calculation method being applicable to various Heusler alloys.

The concentration dependences of $T_C^{\mathrm{expt.}}$ and $T_C^{\mathrm{calc.}}$ are plotted in Fig. 7. In the evaluation of $T_C^{\mathrm{calc.}}$, the effective exchange constant J_0 in each composition was calculated from Eq. (1), and the magnetic interaction was assumed to be ruled over by the magnetic element having the highest value of J_0. It can be seen from Fig. 7 that $T_C^{\mathrm{calc.}}$ is not increased linearly with increasing x, being convex upward, and has a maximum value of 865 K at $x=0.75$, which is qualitatively consistent with the experimental data of $T_C^{\mathrm{expt.}}$, although the magnitude of $T_C^{\mathrm{calc.}}$ is about 100 to 300 K higher than $T_C^{\mathrm{expt.}}$ except for the value of Co_2VGa. Such a discrepancy results from the estimation based on the mean-field approximation.

Kübler discussed the Curie temperature T_C of various magnetic materials.[61] He showed that the order of magnitude T_C for CoNi alloy system is given as $T_C^{\mathrm{MF}} > T_C^{\mathrm{RP}} > T_C^{\mathrm{SF}}$. Here, superscripts MF, RP, and SF stand for the mean-field approximation, random phase approximation, and spin fluctuation approximation, respectively. Experimental values of $T_C^{\mathrm{expt.}}$ for FeNi and CoNi are close to T_C^{RP}, but those for $CoNi_3$ and Mn_2VAl prefer T_C^{MF}.[61] The proof of the relation $T_C^{\mathrm{MF}} > T_C^{\mathrm{RP}}$ for the collinear magnetic state with multiple sublattices was made by Rusz *et al.*[62] For Co_2MnSi, the value of T_C^{MF} calculated by Sasioglu *et al.* comes close to $T_C^{\mathrm{expt.}}$. However, Kübler *et al.* pointed out that their result of T_C^{RP} is very close to $T_C^{\mathrm{expt.}}$.[63] In this manner, the theoretical results sensitively depend on the calculation conditions. At the present stage, it is difficult to say which is more advantageous or not in order to estimate T_C. Although the present method for the estimation of T_C from J_0 is conventional, it is useful to discuss systematically for various alloys.[64]

The value of T_C for the $Co_2(V_{1-x}Mn_x)Ga$ alloys almost linearly increases with increasing x, being different from that

for the $Co_2(Cr_{1-x}Fe_x)Ga$ alloys.[22] In the $Co_2(Cr_{1-x}Fe_x)Ga$ alloys, the hybridization between the Fe-3*d* and Co-3*d* bands enhances the magnetic moment of Co and the value of the spin magnetic moment of Co increases with increasing Fe content.[22] Consequently, the spin magnetic moments of Co for Co_2CrGa and Co_2FeGa alloys are $0.90\mu_B$/atom and $1.19\mu_B$/atom, respectively.[22] In addition, the spin magnetic moment of Fe is almost invariable in the entire range of *x*. On the contrary, in the present $Co_2(V_{1-x}Mn_x)Ga$ alloys, the spin magnetic moment of Co of $0.95\mu_B$/atom at $x=0.0$ decreases to $0.77\mu_B$/atom at $x=1.00$. Furthermore, the spin magnetic moment of Mn also decreases with increasing *x*. These would be the reasons why the concentration dependence of T_C of the $Co_2(V_{1-x}Mn_x)Ga$ alloy system is different from that of the $Co_2(Cr_{1-x}Fe_x)Ga$ alloy system. Finally, it should be noted that $T_C^{\text{expt.}}$ of 615 K for the alloy with $x=0.50$ in the present alloy system $Co_2(V_{1-x}Mn_x)Ga$ is higher than that of Co_2CrGa alloy of 495 K in which the number of the valence electrons corresponds with each other.[21,22]

V. CONCLUSION

The magnetic properties, phase stability, electronic structure, and spin polarization ratio *P* of the $L2_1$-type $Co_2(V_{1-x}Mn_x)Ga$ alloys were systematically investigated from both experimental and theoretical viewpoints. The magnetic and the DSC measurements have been carried out, and the phase stability was discussed, correlating with the order-disorder transition temperature. Furthermore, the DOS, the spin polarization ratio *P*, and the effective exchange constant J_0 have been evaluated by the LMTO-ASA method with the CPA. Main results are summarized as follows:

(1) The saturation magnetic moment M_s at 4.2 K linearly increases with increasing *x*, in good agreement with the GSP rule supported by the total spin magnetic moment obtained from the theoretical calculations.

(2) The order-disorder transition temperature $T_t^{L2_1/B2}$ from the $L2_1$ to *B*2-type phase linearly decreases with increasing *x*, and $T_t^{L2_1/B2}$ of the $Co_2(V_{0.5}Mn_{0.5})Ga$ alloy is higher than that of the Co_2CrGa alloy, exhibiting that the phase stability of the former is higher than that of the latter. The high value of $T_t^{L2_1/B2}$ means that the $L2_1$-type phase is thermally stable, which is practically important for spintronic devices.

(3) The DOS calculated by the LMTO-ASA method exhibits that the spin polarization ratio *P* of the alloy with $x=0.75$ is the highest of about 80% in the present substituted alloys.

(4) The experimental Curie temperature $T_C^{\text{expt.}}$ increases with increasing *x* and exhibits a convex upward with a maximum of about 704 K at $x=0.75$, qualitatively in accordance with the calculated Curie temperature $T_C^{\text{calc.}}$ estimated from the effective exchange constant J_0.

ACKNOWLEDGMENTS

The present work was supported by Grant-in-Aid for Scientific Research from the Ministry of Education, Science, Sports and Culture, Japan, Core Research for Evolutional Science and Technology (CREST), Japan Science and Technology Agency (JST), and by a Grant-in-Aid for Scientific Research (S) No. 18106012 from the Japan Society for the Promotion of Science.

*Corresponding author. rie@tagen.tohoku.ac.jp
†Present address: Technical Division, School of Engineering, Tohoku University, 6-6-11 Aoba-yama, 980-8579 Sendai, Japan.

[1] S. A. Wolf, D. D. Awschalom, R. A. Buhrman, J. M. Daughton, S. von Molnár, M. L. Roukes, A. Y. Chtchelkanova, and D. M. Treger, Science **294**, 1488 (2001).
[2] R. A. de Groot, F. M. Mueller, P. G. van Engen, and K. H. J. Buschow, Phys. Rev. Lett. **50**, 2024 (1983).
[3] J. Kübler, A. R. Williams, and C. B. Sommers, Phys. Rev. B **28**, 1745 (1983).
[4] S. Ishida, S. Sugimura, S. Fujii, and S. Asano, J. Phys.: Condens. Matter **3**, 5793 (1991).
[5] S. Ishida, S. Fujii, D. Kashiwagi, and S. Asano, J. Phys. Soc. Jpn. **64**, 2152 (1995).
[6] I. Galanakis, P. H. Dederichs, and N. Papanikolaou, Phys. Rev. B **66**, 174429 (2002).
[7] I. Galanakis, P. Mavropoulos, and P. H. Dederichs, J. Phys. D **39**, 765 (2006).
[8] A. Kellow, N. E. Fenineche, T. Grosdidier, H. Aourag, and C. Coddet, J. Appl. Phys. **94**, 3292 (2003).
[9] M. P. Raphael, B. Ravel, Q. Huang, M. A. Willard, S. F. Cheng, B. N. Das, R. M. Stroud, K. M. Bussmann, J. H. Claassen, and V. G. Harris, Phys. Rev. B **66**, 104429 (2002).
[10] U. Geiersbach, A. Bergmann, and K. Westerholt, Thin Solid Films **425**, 225 (2003).
[11] H. Kubota, J. Nakata, M. Oogane, Y. Ando, A. Sakuma, and T. Miyazaki, Jpn. J. Appl. Phys., Part 2 **43**, L984 (2004).
[12] Y. Sakuraba, J. Nakata, M. Oogane, Y. Ando, H. Kato, A. Sakuma, T. Miyazaki, and H. Kubota, Appl. Phys. Lett. **88**, 022503 (2006).
[13] N. Tezuka, N. Ikeda, A. Miyazaki, S. Sugimoto, M. Kikuchi, and K. Inomata, Appl. Phys. Lett. **89**, 112514 (2006).
[14] H. J. Elmers, S. Wurmehl, G. H. Fecher, G. Jakob, C. Felser, and G. Schönhense, Appl. Phys. A: Mater. Sci. Process. **79**, 557 (2004).
[15] S. Ishida, S. Kawakami, and S. Asano, Mater. Trans. **45**, 1065 (2004).
[16] Y. Miura, K. Nagao, and M. Shirai, J. Appl. Phys. **95**, 7225 (2004).
[17] K. Inomata, S. Okamura, and N. Tezuka, J. Magn. Magn. Mater. **282**, 269 (2004).
[18] S. Okamura, R. Goto, N. Tezuka, S. Sugimoto, and K. Inomata, Jpn. J. Appl. Phys., Part 1 **28**, 172 (2004).
[19] K. Kobayashi, R. Y. Umetsu, R. Kainuma, K. Ishida, T. Oyamada, R. Kainuma, K. Ishida, R. Y. Umetsu, A. Fujita, and K. Fukamichi, Appl. Phys. Lett. **85**, 4684 (2004).
[20] K. Kobayashi, R. Y. Umetsu, A. Fujita, K. Oikawa, R. Kainuma, K. Fukamichi, and K. Ishida, J. Alloys Compd. **399**, 60 (2005).

[21] R. Y. Umetsu, K. Kobayashi, R. Kainuma, A. Fujita, K. Fukamichi, K. Ishida, and A. Sakuma, Appl. Phys. Lett. **85**, 2011 (2004).
[22] R. Y. Umetsu, K. Kobayashi, A. Fujita, K. Oikawa, R. Kainuma, K. Ishida, N. Endo, K. Fukamichi, and A. Sakuma, Phys. Rev. B **72**, 214412 (2005).
[23] K. Kobayashi, R. Kainuma, and K. Ishida, Mater. Trans. **47**, 20 (2006).
[24] I. Galanakis, J. Phys.: Condens. Matter **16**, 3089 (2004).
[25] Y. Miura, K. Nagao, and M. Shirai, Phys. Rev. B **69**, 144413 (2004).
[26] I. Galanakis, K. Özdoğan, B. Aktaş, and E. Şaşıoğlu, Appl. Phys. Lett. **89**, 042502 (2006).
[27] S. Wurmehl, G. H. Fecher, K. Kroth, F. Kronast, H. A. Dürr, Y. Takeda, Y. Saitoh, K. Kobayashi, H. Lin, G. Schönhense, and C. Felser, J. Phys. D **39**, 803 (2006).
[28] B. Balke, G. H. Fecher, H. C. Kandpal, C. Felser, K. Kobayashi, E. Ikenaga, J.-J. Kim, and S. Ueda, Phys. Rev. B **74**, 104405 (2006).
[29] G. H. Fecher and C. Felser, J. Phys. D **40**, 1582 (2007).
[30] M. Kallmayer, H. J. Elmers, B. Balke, S. Wurmehl, F. Emmerling, G. H. Fecher, and C. Felser, J. Phys. D **39**, 786 (2006).
[31] K. Özdoğan, B. Aktaş, I. Galanakis, and E. Şaşıoğlu, J. Appl. Phys. **101**, 073910 (2007).
[32] K. Ishikawa, Ph.D. thesis, Tohoku University, 2002.
[33] K. Kobayashi, R. Y. Umetsu, K. Ishikawa, R. Kainuma, and K. Ishida, J. Magn. Magn. Mater. **310**, 1794 (2007).
[34] O. K. Andersen, Phys. Rev. B **12**, 3060 (1975).
[35] U. von Barth and L. Hedin, J. Phys. C **5**, 1629 (1972).
[36] J. F. Janak, Solid State Commun. **25**, 53 (1978).
[37] A. Sakuma, J. Phys. Soc. Jpn. **69**, 3072 (2000).
[38] A. I. Liechtenstein, M. I. Katsnelson, and V. A. Gubanov, Solid State Commun. **54**, 327 (1985).
[39] A. P. Malozemoff, A. R. Williams, and V. L. Moruzzi, Phys. Rev. B **29**, 1620 (1984).
[40] J. Kübler, Physica B & C **127**, 257 (1984).
[41] J. Kübler, *Theory of Itinerant Electron Magnetism* (Clarendon, Oxford, 2000).
[42] K. H. J. Buschow and P. G. van Engen, J. Magn. Magn. Mater. **25**, 90 (1981).
[43] P. J. Webster, J. Phys. Chem. Solids **32**, 1221 (1971).
[44] K. Kobayashi, Ph.D. thesis, Tohoku University, 2006.
[45] K. R. A. Ziebeck and P. J. Webster, J. Phys. Chem. Solids **35**, 1 (1974).
[46] K. Ishikawa, I. Ohnuma, R. Kainuma, K. Aoki, and K. Ishida, J. Alloys Compd. **367**, 2 (2004).
[47] N. C. Oforka and B. B. Argent, J. Less-Common Met. **114**, 97 (1985).
[48] N. C. Oforka and C. W. Haworth, Scand. J. Metall. **16**, 184 (1987).
[49] V. S. Gorsky, Z. Phys. **50**, 64 (1928).
[50] W. L. Bragg and E. J. Williams, Proc. R. Soc. London, Ser. A **145**, 699 (1934), **151**, 540 (1935).
[51] G. Inden, Z. Metallkd. **66**, 577 (1975).
[52] H. C. Kandpal, G. H. Fecher, and C. Felser, J. Phys. D **40**, 1507 (2007).
[53] H. C. Kandpal, G. H. Fecher, C. Felser, and G. Schönhense, Phys. Rev. B **73**, 094422 (2006).
[54] J. M. D. Coey and M. Venkatesan, J. Appl. Phys. **91**, 8345 (2002).
[55] C. Felser, G. H. Fecher, and B. Balke, Angew. Chem., Int. Ed. **46**, 668 (2007).
[56] K. Özdoğan, E. Şaşoğlu, B. Aktaş, and I. Galanakis, Phys. Rev. B **74**, 172412 (2006).
[57] M. Sargolzaei, M. Richter, K. Koepernik, I. Opahle, H. Eschrig, and I. Chaplygin, Phys. Rev. B **74**, 224410 (2006).
[58] Y. Kurtulus, M. Gilleßen, and R. Dronskowski, J. Comput. Chem. **27**, 90 (2006).
[59] Y. Sakuraba, J. Nakata, M. Oogane, H. Kubota, and Y. Ando, Jpn. J. Appl. Phys., Part 2 **44L**, 1100 (2005).
[60] Ph. Mavropoulos, K. Sato, R. Zeller, P. H. Dederichs, V. Popescu, and H. Ebert, Phys. Rev. B **69**, 054424 (2004).
[61] J. Kübler, J. Phys.: Condens. Matter **18**, 9795 (2006).
[62] J. Rusz, I. Turek, and M. Diviš, Phys. Rev. B **71**, 174408 (2005).
[63] J. Kübler, G. H. Fecher, and C. Felser, Phys. Rev. B **76**, 024414 (2007).
[64] Y. Kurtulus, R. Dronskowski, G. D. Samolyuk, and V. P. Antropov, Phys. Rev. B **71**, 014425 (2005).